# Spectroscopic Evidence of Interstellar Solid Hydrogen

J. Schaefer
Max-Planck-Institut für Astrophysik,
Karl-Schwarzschild-Strasse 1, 85741 Garching, Germany
e-mail: jas@mpa-garching.mpg.de

November 20, 2006

**Abstract**

Infrared bands observed in the ISO-SWS mission are explained as being emitted from inside hydrogen solids, probably in the relaxation process of recombined $H_2$. Double rotational transitions in solid hydrogen are discussed, and an approximate formalism developed by Van Kranendonk is applied to show the crucial role of the delocalized j = 2 states in the explanation of the observed intensities and widths of zero-phonon bands at wavelengths between 6 and 12 m$\mu$. Emission rates and column densities of the prominent features have been estimated with reasonable accuracy.

# 1. Introduction

The question is raised in this paper whether existing solid hydrogen in the interstellar medium of the Milky Way could be spectroscopically detected. There is no need to wait for forthcoming observations because sufficiently resolved spectra have been provided in the very successful ISO mission (1995-97), in particular the ubiquitous infrared (IR) emission features between 6 and 12 m$\mu$ observed in the Milky Way (at sufficiently large scales) and in other spiral galaxies, however, the commonly accepted interpretation claims these features for mixtures of polycyclic aromatic hydrocarbons (PAHs). Hundreds of publications have been devoted to this subject, reporting theoretical and experimental work. I may mention just one publication discussing this assignment in detail (Boulanger et al., 1998 [1]).

This paper is aimed at showing that the observed features provide spectroscopic evidence also of solid hydrogen sources and by that making a first step of hypothetically introducing solid hydrogen as an existing species in the interstellar medium. So far solid hydrogen cannot be considered as an assigned species because practically nothing is known about the details of recombination of atomic hydrogen in hydrogen solids which is the only thinkable solid hydrogen source of the radiation to be discussed in this paper. So far it is also not certain that solid hydrogen will succeed as an interstellar species in disagreement with opposite commonly accepted convictions of interstellar physics. Nevertheless, there is a chance in my opinion that some people encouraged by this paper start thinking about experimental or theoretical work on solid hydrogen.

Solid hydrogen radiation theory is confined here to the so-called "zero-phonon" bands, the simplest available approximation for this subject. I am going to use this successful approximation described in Van Kranendonk's textbook [2] which neglects all couplings

to the lattice vibrations. Zero-phonon intensities produce the relatively sharp features of the spectra with the characteristic band widths. A short guide through the paper is provided at the end of the Introduction because a majority of the readers is probably not familiar with the very short presentation of the approximate solid hydrogen theory followed in this paper.

Knowledge of solid hydrogen physics has grown rapidly starting at about half a century ago. Experimental work on the interaction of solid hydrogen with radiation has been started in the fifties of last century. Since then it has been exclusively absorption measurements. I may cite here papers of Gush et al. in 1957 [3] and 1960 [4], of Allin et al. in 1958 [5] and of Kiss in 1959 [6]. Theoretical work and especially the explanations of the measurements have been contributed at about the same time by Van Kranendonk and co-workers. I may cite Van Kranendonk 1959 [7] and 1960 [8], Poll and Van Kranendonk 1962 [9] and Van Kranendonk and Karl 1968 [10]. A review of the last four decades has been published by Mishra et al. in 2004 [11]. The essence of the theoretical work is summarized in the textbook on *Solid Hydrogen* published by Van Kranendonk in 1983 [2].

Solid hydrogen is known as a quantum crystal, in which the single molecules can rotate and vibrate almost freely, the rotational and vibrational quantum numbers are very good quantum numbers, and the rotational and vibrational transition frequencies can be determined from the known energy levels of the free $H_2$ molecule within errors of a few wavenumbers. We find normally negative shifts of a few wavenumbers for parahydrogen molecules emitting in the crystal which can be attributed to the slightly different effective $H_2$ potential valid in the crystal. Pure solid hydrogen is parahydrogen, admixed ortho-$H_2$ molecules are understood as point defects, if the abundance of ortho-$H_2$ in the crystal is small. Twelve molecules are surrounding each central molecule at a constant distance, the "nearest neighbor" distance, of (empirical) $R_0 = 7.09\ a_0 = 3.75$ Å(Van Kranendonk [8]). It is larger than the empirically fitted equilibrium distance of 6.5 $a_0$ of two freely interacting ground-state $H_2$ molecules [12]. This shows that the crystal of solid hydrogen is blown up by the zero-point lattice vibrations. Two possible close-packed structures provide different conditions of inversion symmetry in the lattice: the "face-centered cubic" (fcc) and the "hexagonal close-packed" (hcp). Both structures contain monomolecular layers with six nearest neighbors (nns) forming a regular hexagon around each molecule. In following Van Kranendonk [2], I assume the hcp crystal being generally valid, with a unit cell prism containing two $H_2$ molecules.

The next three sections introduce the approximate method used to calculate emission rates of the rigid-lattice zero-phonon bands in parahydrogen solids. It follows from the valid assumption that the main interactions and the dipole moments in the crystal are pairwise additive. Van Kranendonk's theory [2] is used which accounts for the main effects of $H_2$ interactions and dipole moment functions, by that rendering successful explanations of measured absorption coefficients, especially of pair transitions. Accordingly, this method is confined to double rotational transitions of $H_2$ pairs, or at least a second rotating molecule acts as a companion in a single transition. Hence the formal treatment becomes similar to the normally used formalism of two interacting free $H_2$ molecules emitting or absorbing collision induced radiation, but extended with solid state effects and with simplifications caused by symmetry effects. The discussion of symmetry effects is started in the next section with the required zero-order rotationally invariant pair wave functions of pure para-$H_2$ and of mixed ortho-para-$H_2$ pairs.

Section 3 is aimed at introducing to the physics of zero-phonon emission bands of solid hydrogen in the wavelength range between 6 and 12 m$\mu$ explained with pure rotational transitions of pairs of hydrogen molecules in the solid which undergo simultaneous tran-

sitions and emit a single infrared photon. The widths of the bands have been observed with practically constant sizes at all sources covered in the ISO mission which needs an explanation. Another issue are the shifts of the mixed ortho-para pair transition bands caused by the so-called "excess binding energies" of the ortho-$H_2$ impurities in the parahydrogen crystal. Both quantities will be discussed as typical solid hydrogen phenomena, determined by the anisotropic interaction potential of $H_2$ pairs which is approximately known only for the free $H_2$ - $H_2$ pair (Schaefer and Köhler [12]).

Considering symmetry properties of the lattice leads to the main rotational coupling term, the electric quadrupole-quadrupole (EQQ) interaction. It is axially symmetric only for free $H_2$ pairs, but this fits to the chosen approximation. It causes level splitting of the total angular momenta J states of pairs of two rotating molecules at nn distance and the so-called "rotonic profiles" which appear in double rotational transitions with a j = 2 state involved initially and/or finally. The so-called "hopping matrix elements" of the j = 2 state are introduced which give rise to hopping exciton ("roton") effects, essential effects used to explain the observed features. Since the rotational energy S(0) of the j = 2 state is delocalized in that case, also called "hopping through the crystal", I call it sometimes S(0) exciton. Both the localized J splittings at nn distance as well as the rotonic splitting of S(0) excitons summed over pairs with extended distances is briefly introduced. The former is easily calculated and should certainly be done in preparation of calculations of the dipole transition matrix elements of the $|JM>$ states. Examples are also shown in the literature: splitting of the initial Js of ground-state ortho-$H_2$ pairs in orthohydrogen in Van Kranendonk [2], and splitting of final Js of parahydrogen pairs in Mengel et al.[15]. Axial symmetry of the EQQ potential term is assumed in both examples.

Rotating molecules in the lattice are coupled to the lattice vibrations ("spin-lattice coupling") which causes phonon radiation and a small correction of the rotational energy levels by this so-called "self-energy" effect. It has been explained by Van Kranendonk and Sears [16]: the lattice vibrations cause an anisotropic blowing up of the crystal thus providing an anisotropic coupling of rotational motion to the vibrational motion of the neighboring molecules and a weak splitting of the degenerate j levels (Luryi and Van Kranendonk [17]). This is neglected in the calculation of the zero-phonon bands. The basic symmetry requirements of para-$H_2$ pairs prohibit "excess binding energies" in the parahydrogen lattice because the pair interaction potentials between the identical (indistinguishable) molecules are symmetric with regard to the two molecules. This symmetry does not apply to mixed ortho-para pairs which is the fundamental reason for local distortions around ortho-$H_2$ impurities in the parahydrogen lattice. Local distortion means radial forces directed to the ortho-$H_2$ impurities, and consequently self-energies enlarged by "excess binding energies". They will show up in the explained spectrum, in the shifts of mixed ortho-para pair emission bands.

Section 4 adds in the main radiative effects of the pairwise additive induced dipole moment functions as required by the crystal symmetry. An important enhancement of the emission rates caused by the hopping S(0) excitons will be accepted from Van Kranendonk's calculation of the S(0) + S(0) pair absorption coefficient and his comparison with the measurement of Kiss 1959 [6]. At the end of section 4 all details are available to estimate zero-phonon emission band widths and emission rates for double rotational transitions of $H_2$ pairs.

Section 5 starts with the presentation of the observed ISO-SWS spectrum containing the four prominent features which are to be explained. A series of double rotational de-excitations is introduced which fits part of the prominent features, and additional double rotational transitions combining de-excitation and excitation in the $H_2$ pairs complete

the analysis. Only selected double rotational pair transitions are used in the analysis of the spectrum which at least include one delocalized j = 2 state in the initial or final pair states because the S(0) excitons provide the significantly enhanced squared dipole moment matrix elements. Experimentally determined transition energies of single $H_2$ molecules in the solid will be used to estimate the positions of the fitted pure parahydrogen bands. This is inappropriate for the mixed ortho-para pairs because of the energy shifts of the ortho-$H_2$ impurities. Altogether ten rotational transition bands of $H_2$ pairs will be discussed. Additional significant double rotational bands at higher frequencies up to about 3000 $cm^{-1}$ are briefly mentioned in the Discussions.

Averaged column densities of the sources are obtained from the fitted zero-phonon bands in order to show the amount of rotationally excited $H_2$ pairs responsible for the observed radiation, but more details of the recombination of $H_2$ in the solids are certainly needed to obtain estimates of surfaces and masses of hydrogen solids from information found in the observed spectra.

The results of the applied approximate rigid-lattice pair method of calculating zero-phonon bands are discussed in section 6.

# 2. Approximate pair wave functions in the crystal

I briefly recall a few details about hydrogen pair wave functions of free pairs valid in the scattering theory of two interacting $H_2$ molecules (as developed by Takayanagi [18]) which are also used here in the solids as zero-order wave functions. $H_2$ as well as $H_2$ pairs are Bose systems. Accordingly, para-$H_2$ molecules with zero (meaning symmetric) nuclear spin and symmetric ground-state electron spin have only even rotational angular momentum states. The other species, ortho-$H_2$, has nuclear spin one (antisymmetric), again symmetric ground-state electron spin, and consequently only odd, meaning antisymmetric angular momentum states. Whilst the mixed ortho-para $H_2$ pair contains two distinguishable parts of Bose particles, the $H_2$ molecules in pairs of parahydrogen and orthohydrogen at the vibrational ground-state level are indistinguishable with regard to their rotational states, therefore, their pair wave function must be symmetric or antisymmetric under exchange of the two molecules depending upon the nuclear spin of the pair. It follows that parahydrogen pair states (mainly subject of this paper) require symmetric pair wave functions.

The wave functions used in this paper are total J,M eigenfunctions and generally normalized eigenfunction vectors with components separated into radial and angular parts rendering the rotationally invariant coupling of two rotational states $j_1$ and $j_2$ as

$$\Psi^{JM}(\mathbf{R}, \mathbf{r_1}, \mathbf{r_2}; j_1, j_2) = \sum_{jl} R^{-1} \bar{f}^{JM}_{j_1 j_2 jl}(R) I^{JM}_{j_1 j_2 jl}(\hat{\mathbf{r}}_\mathbf{1}, \hat{\mathbf{r}}_\mathbf{2}, \hat{\mathbf{R}}), \tag{1}$$

with

$$\bar{f}^{JM}_{j_1 j_2 jl}(R) = \int dr_1 \chi^2_{j_1}(r_1) \int dr_2 \chi^2_{j_2}(r_2) f^{JM}_{j_1 j_2 jl}(r_1, r_2, R)$$

where the $\mathbf{r}_i$ specify the intramolecular coordinates, $\mathbf{R}$, the collision coordinate, connects the centers of masses of the two molecules, and the $\chi_j(r)$ are normalized radial eigenfunctions of the rotational $H_2$ states. The radial eigenvectors $\bar{f}$ are normalized at the constant

rigid-lattice distances of the $H_2$ molecules :

$$\int dR|\sum_{jl}\bar{f}^{JM}_{j_1j_2jl}(R)|^2\delta(R-R_0)=1,$$

hence $\Psi^{JM}_{j_1j_2}$ is also normalized. The angular part is

$$I^{JM}_{j_1j_2jl}(\hat{\mathbf{r}}_\mathbf{1},\hat{\mathbf{r}}_\mathbf{2},\hat{\mathbf{R}})=\sum_{m_1m_2mm_l}C(j_1j_2j;m_1m_2m)C(jlJ;mm_lM)Y_{j_1m_1}(\hat{\mathbf{r}}_\mathbf{1})Y_{j_2m_2}(\hat{\mathbf{r}}_\mathbf{2})Y_{lm_l}(\hat{\mathbf{R}}),\ (2)$$

where $\hat{\mathbf{r}}=\mathbf{r}/\mathrm{r}$, the Cs are Clebsch-Gordan coefficients, and the Ys are spherical harmonics. It shows the angular momentum coupling in the order of $\mathrm{j}_1+\mathrm{j}_2\rightarrow\mathrm{j}$ and j is coupled with the orbital angular momentum $l$ to total J. Exchange of the molecules gives

$$X_{12}I^{JM}_{j_1j_2jl}=I^{JM}_{j_1j_2jl}(\hat{\mathbf{r}}_\mathbf{2},\hat{\mathbf{r}}_\mathbf{1},-\hat{\mathbf{R}})=(-1)^{j_1+j_2+j+l}I^{JM}_{j_2j_1jl}(\hat{\mathbf{r}}_\mathbf{1},\hat{\mathbf{r}}_\mathbf{2},\hat{\mathbf{R}}),$$

whereas the parity is obtained from $\mathrm{P}_{12}=(\text{-}1)^{j_1+j_2+l}$ which shows that *obviously a change of $l$ is required for rotational dipole transitions*. This is a curiosity of the rigid-lattice pair approximation. Orbiting pairs in the rigid-lattice approximation is unthinkable by all means. We deal with that by assuming that any radiative dipole transition requires $l=0$ initially, and the final orbiting energy is immediately transferred to the lattice, thus contributing to the phonon branches of the bands. It is a plausible assumption because an anisotropic coupling to the lattice vibrations exists.

Symmetric pair wave functions of parahydrogen are established with the symmetrized angular part as

$$I^{JM(s)}_{j_1j_2jl}=[2(1+\delta_{j_1j_2}\delta_{v_1v_2})]^{-1/2}[I^{JM}_{j_1j_2jl}(\hat{\mathbf{r}}_\mathbf{1},\hat{\mathbf{r}}_\mathbf{2},\hat{\mathbf{R}})+(-1)^{j_1+j_2+j+l}I^{JM}_{j_2j_1jl}(\hat{\mathbf{r}}_\mathbf{1},\hat{\mathbf{r}}_\mathbf{2},\hat{\mathbf{R}})].\qquad(3)$$

The two restricted symmetrized products, one for $j_1\leq j_2$ and the other one for $j_2\geq j_1$ are the zero-order wave functions of pure parahydrogen free $(j_1,j_2)$ pairs as well as pairs in the parahydrogen solids. Symmetrization is the basic condition of the physics of parahydrogen pairs, of course including radiation. I show an example: when both $H_2$ states are rotational in the vibrational ground-state, all angular wave functions with $(-1)^{j+l}=$ -1 vanish in the case of $\mathrm{j}_1=\mathrm{j}_2$. Hence the symmetrized pair wave functions of the rotational para-$H_2$ ground-state occur only with even $l$ and J and with positive parity, i.e., the simultaneous dipole emission from the initial pair $(\mathrm{j}_1,\ \mathrm{j}_2)=(2,2)$ with positive parity ($l=0$) to the ground-state pair is forbidden. The observed spectrum provides proof as we will see below.

# 3. Approximate spread and shift of the emission bands

The anisotropic parts of the $H_2$ pair interaction potential determine the spectroscopic properties of solid hydrogen emission bands discussed in this paper. I separate this part from the Hamiltonian and define

$$H=H_0+\sum_{i<j}A(\hat{\mathbf{r}}_\mathbf{i},\hat{\mathbf{r}}_\mathbf{j},\mathbf{R}_\mathbf{ij})\equiv H_0+H_1.\qquad(4)$$

Since the $H_1$ operator of the solid can be reduced by means of symmetry effects not valid in the $H_1$ operator of the free pair, I should first discuss the symmetry effects of the

crystal applied to the pairwise additive interactions in the crystal which are expanded in a rotationally invariant form as

$$V(\mathbf{R_{ij}},\mathbf{r_i},\mathbf{r_j}) = (4\pi)^{3/2}\sum_{l_1l_2K} V_{l_1l_2K}(R_{ij},r_i,r_j)\sum_{m_1m_2m} C(l_1l_2K;m_1m_2m) \times Y_{l_1m_1}(\hat{\mathbf{r}}_\mathbf{i})Y_{l_2m_2}(\hat{\mathbf{r}}_\mathbf{j})Y^*_{Km}(\hat{\mathbf{R}}_\mathbf{ij}). \quad (5)$$

Calculations of potential matrix elements will be done for zero orbiting motion. This reduces the angular part of the pair wave function defined in Eq.2 to the coupled product of two spherical harmonics. It is then appropriate to choose the z-axis of the interaction potential along the $\mathbf{R}_{ij}$ vector yielding

$$V(\mathbf{R_{ij}},\mathbf{r_i},\mathbf{r_j}) = 4\pi\sum_{l_1l_2K} V_{l_1l_2K}(R_{ij},r_i,r_j)\sqrt{2K+1}\sum_{\kappa} C(l_1l_2K;\kappa-\kappa 0) \times Y_{l_1\kappa}(\hat{\mathbf{r}}_\mathbf{i})Y_{l_2-\kappa}(\hat{\mathbf{r}}_\mathbf{j}). \quad (6)$$

This expansion is valid only for isolated pairs, but used in the approximation. Integration over the angular part of the matrix element is obtained by making use of some angular momentum algebra (Edmonds [13] and Flügge [14]) which yields the general formula

$$< \bar{J}\bar{M}\bar{j}_1\bar{j}_2|V_{l_1l_2K}|JMj_1j_2> = V_{l_1l_2K}(R,r_1,r_2)\delta_{M\bar{M}}\sqrt{[l_1][l_2][K][\bar{J}][\bar{j}_1][\bar{j}_2][J][j_1][j_2]} \times \begin{pmatrix} \bar{j}_1 & l_1 & j_1 \\ 0 & 0 & 0 \end{pmatrix}\begin{pmatrix} \bar{j}_2 & l_2 & j_2 \\ 0 & 0 & 0 \end{pmatrix}\begin{pmatrix} \bar{j}_1 & j_1 & l_1 \\ \bar{j}_2 & j_2 & l_2 \\ \bar{J} & J & K \end{pmatrix} \times(-1)^{\bar{j}_1+\bar{j}_2+J-M}C(\bar{J}JK;\bar{M}-M0), \quad (7)$$

where [j] ≡ 2j+1, and the symbols in parentheses are Wigner 3j- and a 9j-symbol. I may note that $\bar{M}$ = M is required.

Properties of the potential terms at distances R ≥ $R_0$ can be briefly summarized as follows. Only even $l_1$ and $l_2$ can occur in the expansion because of the inversion symmetry of the $H_2$ molecule. Anisotropic terms at nn distance and above are mainly determined by interactions of the electric quadrupole moment $Q_2$ of $H_2$, i.e., the approximate interaction used is confined to potential terms with $l_i \leq 2$. Terms with $l_1 + l_2 = 2$ are $V_{202}$ and $V_{022}$. They vanish when summed over all $H_2$ pairs in the undistorted hcp crystal, therefore, they are only needed in the case of local distortion produced by a single ortho-$H_2$ impurity. They are not negligible also when lattice vibration is taken into account. Terms with $l_1 + l_2 = 4$ don't vanish. There are three terms of $l_1 = l_2 = 2$: $V_{220}$, $V_{222}$ and $V_{224}$. Odd Ks are excluded because of inversion symmetry of the $H_2$ pair at the center of mass. The terms $V_{220}$ and $V_{222}$, proportional to $R^{-6}$ asymptotically, are known as rather small, therefore, the electric quadrupole-quadruple interaction term $V_{224}$, the only one proportional to $R^{-5}$ asymptotically and approximately at nn distance, is the potential term which generally contributes most to the specific widths of rotational solid hydrogen bands, and in particular to the energy spread of rotationally excited pair states at nn distance. The radial part of the $V_{224}$ term is (see Eqs. 2.47 and 2.49 in Van Kranendonk [2])

$$V_{224}(R,r_1,r_2) = \frac{\sqrt{70}}{15}\frac{Q_2(r_1)\,Q_2(r_2)}{R^5}. \quad (8)$$

The radial factor can be reduced to $V_{224}(R)$ by using the radially averaged $Q_2(r_1)$ and $Q_2(r_2)$ values published by Hunt et al.[19].

Initial double rotationally excited ($j_1$, $j_2 \neq 0$) zero-order $|JM>$ pair states with $l = 0$ split into components of $|M>$ states because the $V_{22K}$ terms do not conserve the total angular momentum J. Hence these splittings in fact contribute partly to the emission band widths. They will be calculated and results are shown in section 5. The $|M>$ states of the pairs ($j_1$, $j_2$) represent generally linear combinations $X_i$ of the zero-order $|JM>$ states calculated by solving the eigenvalue problem

$$\sum_{i'} < V_{224} >_{ii'} X_{i'} = \epsilon_i X_i,$$

with the matrix elements of the approximate Hamiltonian $H_1$, viz.

$$< V_{224} >_{ii'} = < \Psi^{J_i M}(j_1 j_2) | V_{224} | \Psi^{J_{i'} M}(j_1 j_2) >,$$

yielding shifts of the $|JM>$ states for each eigenvalue $\epsilon_i$ and each $|M>$ state. This approximate splitting vanishes generally for a zero $j_i$ in the pair because of the required selection rules expressed in the 3j-Wigner symbols of Eq.7. The only exception is due to the symmetrization of the wave function as shown below in Eq.11.

Assuming also a rigid-lattice splitting for the final $< J'M'|$ states of the infrared double-rotational dipole transition needs a different treatment because the double rotational dipole transitions require a final-state orbital angular momentum $l'$ (= 3, see section 4). As shown in the above section, this kind of artificial effect of the pair approximation seems to be unavoidable. The splitting of the final $< JMj_1j_2jl = 3|$ states at nn distance needs then application of the more general Eq.5 of the interaction potential, and the integration over the angular part of the matrix element gives the general formula

$$\begin{aligned} < \bar{J}\bar{M}\bar{j}_1\bar{j}_2\bar{l} | V_{224} | JMj_1j_2l > \;=\; & V_{224}(R)\delta_{\bar{M}M} 45 \sqrt{[\bar{J}][\bar{j}_1][\bar{j}_2][\bar{l}][J][j_1][j_2][l]} \\ & \times (-1)^{\bar{j}_1+\bar{j}_2+\bar{l}} \begin{pmatrix} \bar{j}_1 & 2 & j_1 \\ 0 & 0 & 0 \end{pmatrix} \begin{pmatrix} \bar{j}_2 & 2 & j_2 \\ 0 & 0 & 0 \end{pmatrix} \begin{pmatrix} \bar{l} & 4 & l \\ 0 & 0 & 0 \end{pmatrix} \\ & \times \sum_{\bar{j}j} \sqrt{[\bar{j}][j]} \begin{pmatrix} \bar{j}_1 & j_1 & 2 \\ \bar{j}_2 & j_2 & 2 \\ \bar{j} & j & 4 \end{pmatrix} \sum_d \begin{pmatrix} \bar{j} & j & 4 \\ \bar{l} & l & 4 \\ \bar{J} & J & d \end{pmatrix} \\ & \times (-1)^{J-M} C(\bar{J}Jd; \bar{M} - M0) \sum_\kappa (-1)^\kappa C(44d; \kappa - \kappa 0) \end{aligned} \tag{9}$$

with $\bar{l} = l = 3$. Again there is normally no rigid-lattice splitting, if one of the $j_i$s is zero, with the exception of the final state of the S(2) + S(0) double rotational de-excitation, as shown in section 5. The splitting of the final $< JM|$ states will be calculated with the same procedure as shown above.

The largest contribution to the band widths, by far more significant than all local $|JM>$ splittings, is made by the energy spread of a j = 2 state molecule in the surrounding parahydrogen crystal. Since this effect provides crucial data for the analysis of the spectrum, the formalism is briefly sketched here by following Van Kranendonk [2].

To begin with, I calculate the matrix element of the Hamiltonian $H_1$, reduced to the EQQ interaction, with a symmetrized zero-order eigenfunction of $H_0$ of a ($j_1$, $j_2$) = (0,2) pair state as defined in section 2, yielding (M ≡ m)

$$\begin{aligned} < \Psi_{02}^{2,\bar{m}} | H_1 | \Psi_{02}^{2m} > \;\approx\; & \int dR |\bar{f}_{02}^{2m}(R)|^2 V_{224}(R) \delta(R - R_0) \\ & \times \int d\hat{\mathbf{r}}_\mathbf{1} d\hat{\mathbf{r}}_\mathbf{2} d\hat{\mathbf{R}} I_{02}^{2m} V_{224}(\hat{\mathbf{R}}, \hat{\mathbf{r}}_\mathbf{1}, \hat{\mathbf{r}}_\mathbf{2}) I_{20}^{2m}, \end{aligned} \tag{10}$$

where $|\bar{f}_{02}^{2m}(R)|^2 = 1$ at nn distance, and the R-dependent EQQ term is obtained with

$$Q_2(r_i) \equiv \int dr_i \chi_0(r_i) Q_2(r_i) \chi_2(r_i) = 0.48515 e a_0^2$$

(Hunt et al.[19]). I may emphasize the exchange of the js in the angular functions of the second factor of Eq.10. The symmetrization of the wave function is needed for a non-vanishing matrix element of $V_{224}$ derived from Eqs.7 and 8. The second term on the right side of Eq.10 yields

$$\begin{aligned} < J\bar{m}02|V_{224}(\hat{\mathbf{R}}, \hat{\mathbf{r}}_\mathbf{1}, \hat{\mathbf{r}}_\mathbf{2})|Jm20 > &= \delta_{m\bar{m}} 3 \cdot 5^3 (-1)^m C(224; \bar{m} - m0) \\ &\times \begin{pmatrix} 0 & 2 & 2 \\ 0 & 0 & 0 \end{pmatrix} \begin{pmatrix} 2 & 2 & 0 \\ 0 & 0 & 0 \end{pmatrix} \begin{pmatrix} 0 & 2 & 2 \\ 2 & 0 & 2 \\ 2 & 2 & 4 \end{pmatrix} \\ &= \delta_{m\bar{m}} 3 (-1)^m C(224; \bar{m} - m0), \end{aligned} \tag{11}$$

and with Eq.8 this gives

$$< \Psi_{02}^{2,\bar{m}} | V_{224} | \Psi_{02}^{2m} >= \sqrt{70} \frac{Q_2(r_1) Q_2(r_2)}{5 R_0^5} (-1)^m C(224; \bar{m} - m0). \tag{12}$$

The next step introduces the "delocalized" j = 2 states. From Bose-Einstein statistics follows that molecules of parahydrogen j = 2 states are indistinguishable not only in a pair state but also in the surrounding parahydrogen crystal of N molecules, i.e., they are delocalized. If the molecule in $\mathbf{R}_i$ is in the rotational state j = 2 with $j_z$ = m, where m = 2, 1, 0, -1, -2, and all other molecules are in the ground-state, there are 5N zero-order eigenstates of a noninteracting rigid lattice Hamiltonian in the crystal,

$$|\Phi^{2m}(\mathbf{R}_i) >= |\Phi^{2m}(r_i, \hat{\mathbf{r}}_i) >= \chi_2(r_i) Y_{2m}(\hat{\mathbf{r}}_i) \prod_{j \neq i}^{N} \chi_0(r_j) Y_{00}(\hat{\mathbf{r}}_j). \tag{13}$$

When the Hamiltonian $H_1$ is switched on with pair interactions of the type $V_{224}$, the correct zero-order pair wave functions must be symmetrized according to the Bose-Einstein statistics and may be written in the form

$$| \ >= \sum_{i=1}^{N} \sum_{m=-2}^{+2} |\Psi_{02}^{2m}(\mathbf{R_i}) >, \tag{14}$$

where $\mathbf{R}_i$ is the position of the j = 2 state in a chosen $H_2$ pair with its definite position of the nn j = 0 state molecule, and the wave equation $H_1| \ >= E| \ >$ is given by

$$\sum_{j \neq i}^{N} \sum_{n} < \Psi_{02}^{2m}(\mathbf{R_i}) | H_1 | \Psi_{02}^{2n}(\mathbf{R_j}) > \Psi_{02}^{2n}(\mathbf{R_j}) = E \Psi_{02}^{2m}(\mathbf{R_i}). \tag{15}$$

The $\Psi_{02}^{2m}(\mathbf{R_i})$ is the "exciton wave function", describing the hopping motion of the j = 2 excitation energy S(0) through the lattice, $|\Psi_{02}^{2m}(\mathbf{R_i})|^2$ is the probability of finding the S(0) excitation in the pair at $\mathbf{R_i}$, with $j_{iz}$ = m. The main contribution to the matrix element in Eq.15 comes from the EQQ interaction and is known as the so-called "hopping matrix element". Eq.12 slightly modified by considering the expansion Eq.5 gives

$$\begin{aligned} < \Psi_{02}^{2\bar{m}}(\mathbf{R_j}) | V_{224} | \Psi_{02}^{2n}(\mathbf{R_i}) > &= \sqrt{70} \frac{Q_2(r_1) Q_2(r_2)}{5 R_{ij}^5} (-1)^m C(224; \bar{m} - n(\bar{m} - n)) \\ &\times \frac{\sqrt{4\pi}}{3} Y_{4(n-\bar{m})}(\hat{\mathbf{R}}_{ij}). \end{aligned} \tag{16}$$

.

Selection rules required for the hopping matrix element are derivable from the Wigner symbols in Eq.11: as long as the approximation is confined to the EQQ interaction, the S(0) exciton is the only hopping "roton" because the ground-state para-$H_2$ molecules can only be excited by this energy quantum. Eq.16 is still valid for the combined "vibron-roton" 1-0 S(0) hopping, but the radial part in Eq.16 is then reduced by a factor of roughly 36 because of the different quadrupole averaging. A $U_0(0)$ ($\Delta$ j = 4) exciton hopping would need $V_{44K}$ terms which are known to be significantly smaller than $V_{224}$ and negligible.

In the third step I show the physical consequences of the hopping S(0) exciton. Proceeding with an application to the fcc lattice, we can see that the $|\Psi_{02}^{2m}(\mathbf{R_i}) >$ states of Eq.15 fulfill the requirement of the Bloch theorem, i.e., there exists a wavevector $\mathbf{k}$ in the reciprocal lattice for each $\mathbf{R}_i$ and a function $\Psi_{02}^{2m}(\mathbf{R})$ periodic in the lattice such that

$$\Psi_{02}^{2m}(\mathbf{R_i} + \mathbf{R}) = \Psi_{02}^{2m}(\mathbf{R})$$

for all $\mathbf{R}_i$ in the lattice such that the wave function of the lattice is of the form

$$\Psi_{02}^{2m}(\mathbf{R_i}) = A_m(\mathbf{k}) exp\{i\mathbf{k} \cdot \mathbf{R_i}\}. \tag{17}$$

.

The amplitudes $A_m(\mathbf{k})$ are solutions of the 5 × 5 secular equation

$$\sum_n H_{mn}(\mathbf{k}) A_n(\mathbf{k}) = E(\mathbf{k}) A_m(\mathbf{k}), \tag{18}$$

where

$$\begin{aligned} H_{mn}(\mathbf{k}) &= \sum_{j \neq i}^{N} < \Psi_{02}^{2m}(\mathbf{R_i}) | H_1 | \Psi_{02}^{2n}(\mathbf{R_j}) > exp\{i\mathbf{k} \cdot (\mathbf{R_j} - \mathbf{R_i})\} \qquad (19) \\ &\approx \sqrt{70}\, \frac{Q_2(r_1) Q_2(r_2)}{5 R_0^5} (-1)^m\, C(224; n - m(n-m)) S_{n-m}(\mathbf{k}; \mathbf{R}_\rho), \end{aligned}$$

with

$$S_\mu(\mathbf{k}; \mathbf{R}_\rho) = \sum_\rho{}' \left(\frac{R_0}{R_\rho}\right)^5 \frac{\sqrt{4\pi}}{3} Y_{4\mu}(\hat{\mathbf{R}}_\rho) exp\{i\mathbf{k} \cdot \mathbf{R}_\rho\} \tag{20}$$

The E($\mathbf{k}$) in Eq.18 determine the band width of the delocalized j = 2 state. As to my knowledge, a serious attempt to solve Eq.18 numerically for arbitrary $\mathbf{k}$ has not been done yet. Approximate useful methods have been introduced by Van Kranendonk [2], but details of this are not discussed here. An estimate has been obtained by Van Kranendonk [2] for a single j = 2 state in the hcp lattice. It needs a slightly modified Eq.18 because there are two molecules instead of one in the unit cell of the hcp crystal. Van Kranendonk assumed a rectangular band shape and calculated the mean square value of the band energies E($\mathbf{k}$) (section 4.2.1 and Appendix B in [2]). This evaluation uses synchronously rotating j = 2 state molecules produced in EQQ interaction at scale sizes which by far exceed the nn distance $R_0$. Their phases are determined by the Bloch theorem. Van Kranendonk estimated a band width of $\approx$ 25 $cm^{-1}$ for a single j = 2 state. It is reduced by about 5-10% by the phonon normalization and is "in order-of-magnitude agreement with the available experimental data"(Van Kranendonk sec.4.2 in [2]). Twice this band

width is valid for the ($j_1$,$j_2$) = (2,2) pair. The doubling of the width is understandable because "two j = 2 rotons are created with arbitrary wave vectors **k** and **-k** producing an absorption band with a total extent equal to twice the width of the j = 2 band." (Van Kranendonk, sec.4.4 in [2]). This has been indeed found experimentally. Proof for the single j = 2 width has been provided by the measurements of the S(0) + S(1) absorption coefficient (Balasubramanian et al. [20]).

These width values are crucial data for the analysis of the spectrum. *It will be generally assumed that each initial and/or final j = 2 state at the vibrational $H_2$ ground-state level (v = 0), occuring in a rotational pair transition in the parahydrogen lattice, contributes with ≈ 20 $cm^{-1}$ to the width of this band.*

Single excited rotational j ≠ 2 states in the ground-state parahydrogen lattice are assumed to be localized on a central molecule, and the anisotropic interaction with the surrounding lattice molecules is only of the type $V_{\lambda 0 \lambda}$, i.e., relatively weak and basically $\propto R^{-6}$ asymptotically and at $R_0$. It cancels out in undistorted parahydrogen hcp ctystals. Additionally, there is a small downward shift of the rotational level called "self-energy" of the spin j molecule caused by the anisotropic "spin-lattice coupling ". The rigid-lattice pair approximation neglects all this for single excited para-$H_2$ j states.

Single ortho-$H_2$ impurities are substitutionally included in the parahydrogen lattice and cause a local distortion of the surrounding lattice molecules in a normally slow migration process. As a result, the ortho-$H_2$ j state gets an "excess binding energy" which is equal to the elastic deformation energy of the surrounding lattice. I may generally assume dipole transition rates of $H_2$ and $H_2$ pairs being small enough in solid hydrogen to normally complete the migration process of the initial state prior to radiation, whereas the migration process of the final states starts up after radiation, therefore, only the "excess binding energies" of the initial states produce a shift of the transition frequency. In more detail, the 2j+1 possible orientations of an ortho j state in the lattice give rise to generally 2j + 1 different local distortions with $R_{ij}$ distances ≠ $R_0$, as determined by the orientation-dependent interaction. The "excess binding energies" must be evaluated for each orientation, from the potentials summed over the $\mathbf{R}_{ij}$ interactions and finally averaged over the j degeneracy. The part of the interaction energy between molecules in the crystal depending on the ($m_j$) orientation of only one single (ortho-$H_2$) molecule is usually called "crystal field interaction".

Two absorption spectra show a negligible "excess binding energy" of the j = 1 state in the ground-state parahydrogen lattice, the S(1) line measured by Mengel et al.[15], and the pair band S(0) + S(1) measured by Balasubramanian et al.[20]. As I have just explained, this is the only "excess binding energy" as yet observed and discussed theoretically because research of solid hydrogen radiation has been strictly confined to absorption. The positions of the nn molecules around the j = 1 impurity have been calculated in distortion and are shown in Fig. 1 in Raich and Kanney [21]. It shows shorter and larger $R_{ij}$ distances of the nn molecules compared to $R_0$.

Since the "excess binding energies" of the single ortho-$H_2$ impurities are caused by the anisotropic interactions with the surrounding crystal molecules, they should become significant in the emission spectra of mixed ortho-para pairs, when the EQQ interaction plays a dominating role again, similar to the emission band widths. For the simplest case, rotationally excited single ortho-$H_2$ j states in the ground-state parahydrogen lattice, there is no EQQ coupling with the lattice molecules, the splitting of the total J states is negligible and the distortion of the $m_j$ orientations is small again ($\propto R^{-6}$). The most significant band widths as well as large "excess binding energies" can be expected for mixed ortho-para pairs containing an excited ortho-$H_2$ j state and a delocalized j = 2

state, where contributions to the effective band widths as well as to the averaged "excess binding energies" have to be summed over the distortions of the lattice which exceed by far the range of the next shell around the ortho-$H_2$ impurity. Efforts of doing this computationally have not yet been started.

# 4. Solid state dipole moment functions

Solid hydrogen emits and absorbs dipole radiation which is almost entirely made by the quadrupole induction mechanism, i.e., the quadrupole $Q_2$ of molecule 1 polarizes molecule 2 with its isotropic polarizibility $\alpha$, the dipole moment is located on molecule 2, but it depends upon the orientation of molecule 1. In a good approximation the dipole moments in the solid are additive: $\vec{\mu} = \sum_{i=1<j}^{N} \vec{\mu}_{ij}$, and the transition rates - of single $\Delta$ j = 2 transitions - are proportional to the square of the sum of all dipole moment matrix elments, where the sum is over all neighboring molecules, not only the nns.

Van Kranendonk's approximation is now applied to the general rotationally invariant spherical expansion of the induced dipole moment function of an $H_2$ pair reading

$$\begin{aligned} \mu_\nu(\mathbf{R_{ij}}, \mathbf{r_i}, \mathbf{r_j}) &= \frac{(4\pi)^{3/2}}{\sqrt{3}} \sum_{\lambda_1\lambda_2\Lambda L} D_{\lambda_1\lambda_2\Lambda L}(R_{ij}, r_i, r_j) \\ &\times \sum_{m_1 m_2 M} C(\lambda_1\lambda_2\Lambda; m_1, m_2, m_1+m_2) C(\Lambda L 1; m_1+m_2, M, \nu) \\ &\times Y_{\lambda_1 m_1}(\hat{r}_i) Y_{\lambda_2 m_2}(\hat{r}_j) Y_{LM}(\hat{R}_{ij}), \end{aligned} \tag{21}$$

where the symbols C and Y are the same as already explained in section 2. Only even $\lambda_i$ can occur in the expansion because of the inversion symmetry of the $H_2$ molecule.

The approximate method neglects all higher order multipole induction terms and reduces the expansion to quadrupole induction which yields $\lambda_1 + \lambda_2 = 2$ and 4. The $D_{022L}$ and the $D_{202L}$ term are the leading terms for an isolated $H_2$ pair, but not so in the solid. They determine mainly single rotational transitions in the gas which differ significantly in intensity compared to rotational transitions in the crystal. This is easily understood: since the molecules surrounding a rotating quadrupole of a single j $\neq$ 0 state are all induced by this same quadrupole, their dipole moments rotate synchronously with the central quadrupole, and the dipole moment there is equal to the sum of the induced dipole moments around, each one $\propto \alpha Q_2$, where $\alpha$ is the isotropic polarizibility. But the dipole moments of molecules diametrically opposite to the central rotating molecule cancel. Since emission and absorption intensities of single $\Delta$j = 2 transitions are proportional to the squared sum of the induced dipole moment matrix elements, they are reduced by this so-called "cancellation effect". The cancellation is total in a perfect fcc crystal. By contrast, double rotational transitions determined by the $D_{22\Lambda L}$ terms and $\propto \gamma Q_2$, with the anisotropic polarizibility $\gamma$, are not affected and are therefore much stronger in the hcp crystal than single transitions (Van Kranendonk [2]). I conclude from that: *double rotational transitions should also dominate the relaxation spectra of the recombined $H_2$ molecules in solid hydrogen.*

More specific details of solid hydrogen radiation can be found by looking at the approximate matrix element of double rotational dipole transitions, from fixed lattice $|JMj_1j_2jl = 0>$ states to general $< J'M'j_1'j_2'j'l'|$ states. Infrared active rotational levels require $\mathbf{k} = 0$ in the case of contributing delocalized j = 2 states. Integration over the

angles and the intramolecular distances gives

$$
\begin{aligned}
< J'M'|\mu_\nu|JM > \;=\; & \sum_\Lambda \int dr_1 dr_2 \chi_{j'1}(r_1)\chi_{j'2}(r_2) D_{22\Lambda L}(r_1,r_2,R)\chi_{j1}(r_1)\chi_{j2}(r_2) \quad (22)\\
& \times 5\sqrt{[\Lambda][L][j_1'][j_2'][J'][j_1][j_2][J]}\\
& \times(-)^{j_1'+j_2'+l'+J'} \begin{pmatrix} j_1' & 2 & j_1 \\ 0 & 0 & 0 \end{pmatrix} \begin{pmatrix} j_2' & 2 & j_2 \\ 0 & 0 & 0 \end{pmatrix} \begin{pmatrix} l' & L & 0 \\ 0 & 0 & 0 \end{pmatrix}\\
& \times(-)^{\Lambda+L+J} \sum_{j'} \sqrt{[j']} \begin{pmatrix} J' & J & 1 \\ \Lambda & L & j' \end{pmatrix} \begin{pmatrix} j_1' & j_1 & 2 \\ j_2' & j_2 & 2 \\ j' & J & \Lambda \end{pmatrix}\\
& \times(-1)^{J'-M+\nu} \begin{pmatrix} J' & J & 1 \\ M' & -M & -\nu \end{pmatrix}
\end{aligned}
$$

with 3-j, 6-j and 9-j Wigner symbols in the parentheses.

Since dipole transitions occur between states of different parity and we assume initially zero orbiting motion, the 3-j symbol of the triple $\{l'L0\}$ in the third row of Eq.22 requires odd $l'$ and odd L = 1 or 3, but only L = 3 ( and $l' = 3$ !) remains because of the crystal symmetry (Van Kranendonk[8]), and the triangle $\{\Lambda$ L 1$\}$ in Eq.22 yields three $\Lambda$s: 2, 3 and 4. An additional result of Eq.22 can be derived from the two other 3j-symbols: there exist also single rotational transitions determined by the $D_{22\Lambda L}$ term under the request that the emitting molecule is paired with a rotating molecule at nn distance.

The integral in Eq.(22) contributes the radial parts of the dipole moment of an $H_2$ pair mutually induced by the electric field of the quadrupole moments. They decrease $\propto R^{-4}$ at large distances and are determined by the anisotropic polarizibility $\gamma$ and the quadrupole moment $Q_2$ yielding (Tipping and Poll [22])

$$B_{2223}(R) \;\rightarrow\; \sqrt{\frac{2}{105}}(\gamma^{(1)}Q_2^{(2)} - Q_2^{(1)}\gamma^{(2)})R^{-4}, \tag{23}$$

$$B_{2233}(R) \;\rightarrow\; -\sqrt{\frac{2}{15}}(\gamma^{(1)}Q_2^{(2)} + Q_2^{(1)}\gamma^{(2)})R^{-4}, \tag{24}$$

$$B_{2243}(R) \;\rightarrow\; \sqrt{\frac{18}{35}}(\gamma^{(1)}Q_2^{(2)} - Q_2^{(1)}\gamma^{(2)})R^{-4}, \tag{25}$$

where the abbreviations (i) have been used to distinguish between matrix elements of $\gamma$ and $Q_2$ of the two $H_2$ molecules, obtained by averaging over the intramolecular distances of the initial $|j_i\rangle$ and final $\langle j_i'|$ rotational states. The averaged values can again be found in the tables published by Hunt et al.[19].

I will neglect contributions from $B_{2223}$ and $B_{2243}$ because they make less than 1% of $B_{2233}$, therefore, only the $D_{2233}$ term of Eq.21 integrated over the angles with $B_{2233}$(R) remains in the applications of dipole moment expansion.

The application of double rotational pair transitions in emission will be further confined to pairs which start from or end with a delocalized j = 2 state molecule. To show the reason for this, I refer to Van Kranendonk's [8] first application of the zero-phonon formalism to a double rotational pair transitions, i.e., the calculation of the absorption coefficient of the S(0) + S(0) transition and the comparison with the measurement done

by Kiss [6]. The double effective width of $\approx 40$ cm$^{-1}$ has already been mentioned above. The second important effect of the delocalized j = 2 states is a "lattice sum" $S_2 = 12.8$ providing an enhancement of the squared dipole moment matrix element of this transition, as calculated by Van Kranendonk by using the summation method of Nijboer and De Wette [23] to include the induction in about two to three hundred neighbors of the final $(j_1, j_2) = (2,2)$ state. A curiosity of this comparison between theory and experiment should be mentioned here regarding the width of the absorption band. Van Kranendonk found a band width of $\approx 40 - 45$ cm$^{-1}$ in the measured spectrum of Kiss [6], whereas Mengel et al. [15] published a FWHM of 28 cm$^{-1}$ obtained from the same spectrum. It does not mean a contradiction because the profile of the band is not Gaussian, neither symmetric. By taking advantage from Van Kranendonk's calculations, *I may assume below roughly half of the effective $S_2$ factor for double rotational transitions with only one j = 2 state starting initially or ending finally* because then the sum runs over half the number of pairs containing a j = 2 state molecule.

In summary: interaction with the S(0) excitons gives a spread of pair energy of $\approx 20$ cm$^{-1}$ for each j = 2 molecule in the pair initially or finally, by that determining mainly the widths of the zero-phonon emission bandes. And a lattice factor of 6.2 is applied to the squared dipole moment matrix elements for each starting or ending j = 2 state in the double pair transition. Consequently, double rotational transitions not including a j = 2 state molecule are smaller by this factor and are expected to occur normally in the background.

The computational procedure of estimating band emission profiles of double rotational transitions starts with the calculation of the initial and final JM components of the local EQQ splitting and their shifts as described in section 3. Eqs. 22 and 24 are then applied to determine squared dipole moment matrix elements $| < J'M'j_1'j_2'|\mu_\nu|JMj_1j_2 > |^2$ of each J$\rightarrow$ J' = J $\pm$ 0,1 transition with their resulting local shifts. The correct zero-phonon approximation would then continue with the calculation of the effective band width and the effective "lattice sum" of each JM transition caused by the delocalized j = 2 state. Programms for this are not available, therefore, the provisional estimates of 20 (40) wavenumbers for the effective width and an enhancement factor of 6.4 (12.8) are used to obtain the contribution of each squared matrix element to the band profile of the pair transition with an assumed Gaussian profile placed at the (experimental) band transition frequency corrected by the resulting local EQQ shift.

Using an intermediate expression for the sum over the magnetic quantum numbers and the polarizations (Condon and Shortley [24]) :

$$| < j_1'j_2'|\vec{\mu}|j_1j_2J > |^2 = \frac{1}{(2J+1)} \sum_{J'} \sum_{M'M\nu} | < J'M'j_1'j_2'|\mu_\nu|JMj_1j_2 > |^2, \qquad (26)$$

the emission rate of the zero-phonon band is then

$$A(j_1'j_2' \leftarrow j_1j_2) = \frac{32\pi^3}{3} \frac{\Delta E^3}{h^3c^3} \frac{e^2}{\hbar} \frac{a_0^2}{(2j_1+1)(2j_2+1)} \sum_J | < j_1'j_2'|\vec{\mu}|j_1j_2J > |^2. \qquad (27)$$

# 5. Spectroscopy of double rotational transitions

All tools are now available for a discussion of the radiation from hydrogen solids observed in the ISO mission, as e.g. at the prominent Photo-Dissociation-Region (PDR) of the

NGC7023 nebula. It is one of the available regions where a sufficient amount of atomic hydrogen is produced by the incident radiation field to recombine partly in the solids, i.e., where solid hydrogen as a relatively weak source, meaning a huge amount of hydrogen solids of unknown sizes, becomes observable in the interstellar space according to the hypothesis. I assume steady recombination of atomic hydrogen in the hydrogen solids at temperatures below the triple point of 13.8 Kelvin. It is plausible to further assume that a great part of the $H_2$ binding energy is collisionally transferred to surrounding lattice molecules prior to restoration of the crystal structure. The result is a much smaller ratio of excited ortho/para $H_2$ abundances after recombination than the statistical ratio of 3:1. The last steps of radiative relaxation are expected to be double rotational transitions at zero vibrational level to be discussed in the frequency range of the ISO-SWS.

A series of double rotational de-excitations is established with the basic rule which requires frequency steps of roughly four times the rotational constant B of $H_2$ for the bands. The series starts with the lowest possible rotational double at the vibrational ground-state level (v = 0), i.e., the S(0) + S(0) emission with the frequency of 710 $cm^{-1}$ ($\approx$ 12 B). Next in the series is the mixed ortho-para double transition S(0) + S(1) with $\approx$ 16 B (plus strong distortion, crystal field interaction and a significant excess binding energy of the j = 3 molecule), next are two double rotational transitions with $\approx$ 20 B, namely the pure para-$H_2$ double S(0) + S(2) and the pure ortho-$H_2$ double S(1) + S(1), etc.

The frequency positions of the bands are taken from the transition frequencies of isolated $H_2$ molecules in solid hydrogen observed with multipole absorption lines (Table 1). The measurements have been obviously applied to ground-state crystals by Balasubramanian et.al. [20, 25], Bountempo et al. [26], Okomura et al.[27], Steinhoff et al.[28] and Mengel et al.[15]. It means that the para-$H_2$ transition frequencies can be simply obtained from the energy differences of the $S_0$, $U_0$, $W_0$ and $Y_0$ transitions, and pure para-$H_2$ pair transition frequencies are simply determined by the sum of the $\Delta j = 2$ energies. There is a general problem arising from the fact that, on the contrary, the energy differences of the ortho-$H_2$ species observed in absorption as single impurities or mixed ortho-para pairs, don't show the excess binding energies of the upper states because the migration of the impurities is slow (Van Kranendonk [2], sec.6) and starts after absorption. Hence the theoretical emission frequency positions of the mixed ortho-para pairs are uncertain by a significant amount of wavenumbers, as long as the computational results of the local distortions and excess binding energies are missing.

The ISO-SWS spectrum of the NGC7023 nebula shows the details (Fig.1). First to be mentioned are the nicely resolved gas phase quadrupole transition lines of $H_2$ emitted in the low-density gas regions of this prominent PDR, ranging from 0-0 S(1) up to 0-0 S(5). They are emitted from locally separated low-density gas sources because collisional relaxation of excited $H_2$ interacting with $H_2$ or H prevails already at reasonable gas densities much smaller then those above the solids.

There are four features to be explained by using ten bands of double rotational transitions of $H_2$ pairs as listed in Table 2. One band is a single S(4) transition band of a double rotationally excited pair. Six of the transitions mentioned in Table 2 follow the basic rule of the series, i.e., they are double rotational de-excitations, three transitions of para-para pairs contribute with a combined de-excitation plus excitation, also a double rotational transition. Seven of the listed pair bands are para-para $H_2$ bands, and a brief comparison of their frequencies with the positions of the observed features makes solid hydrogen a hot candidate for the source. All ten relevant transitions contain hopping S(0) excitons, either in the initial or in the final pair state or in both, hence providing the required band

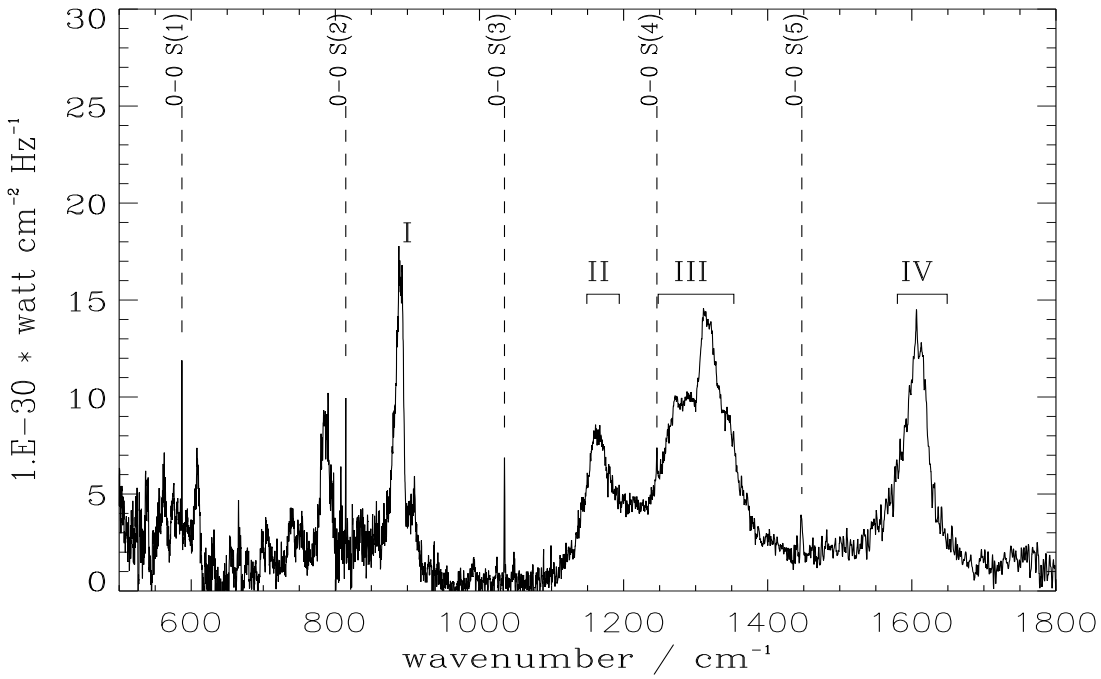


Figure 1:

Table 1: Empirical rotational $\Delta$ j = 2 transitions of $H_2$ in solid hydrogen used in the fits of the ISO-SWS bands. Two values marked with * are obtained from an empirically fitted interaction potential of free $H_2$.

| transition | E/ $cm^{-1}$ |
|---|---|
| 0-0 S(0) | 355.6±0.1 [24,25] |
| 0-0 S(1) | 585.4 [15] |
| 0-0 S(2) | 811.5 [24] |
| 0-0 S(3) | 1033.7 [18] |
| 0-0 S(4) | 1243.44 [26] |
| 0-0 S(5) | 1444.57 [27] |
| 0-0 S(6) | 1633.78 [27] |
| 0-0 S(7) | 1814.624 * |
| 0-0 S(8) | 1979.123 * |

Table 2: De-excitation frequencies of double rotational transitions in $H_2$ pair systems applied to solid hydrogen. The unknown excess binding energies of the ortho-$H_2$ impurities in the mixed ortho-para pairs are indicated with an x.

| no. | transition | $\Delta$ E [$cm^{-1}$] |
|---|---|---|
| **I** | 0-0 S(1) + 0-0 S(0) | 941.47 – x |
| | 0-0 S(4) – 0-0 S(0) | 887.84 (exp.) |
| **II** | 0-0 S(2) + 0-0 S(0) | 1167.1 (exp.) |
| | 0-0 S(4) with a j = 2 host | 1243.4 (exp.) |
| **III** | 0-0 S(6) – 0-0 S(0) | 1278.18 (exp.) |
| | 0-0 S(3) + 0-0 S(0) | 1389.14 – x |
| | 0-0 S(1) + 0-0 S(2) | 1396.9 – x |
| **IV** | 0-0 S(4) + 0-0 S(0) | 1599. (exp.) |
| | 0-0 S(2) + 0-0 S(2) | 1623.0 (exp.) |
| | 0-0 S(8) – 0-0 S(0) | 1625.* |

widths of the features. The graphical fits of the ten bands are shown in Fig. 2.

A description of the results found in the fit procedure may be started with the seven pure parahydrogen transitions. Calculations of the band profiles have been done as described at the end of section 4. The sum of the local splittings of the initial and final pair states determine an approximate small energy correction of the pair transition energies obtained from experimental multipole lines. The lower and upper bounds of the local splitting energies are shown in Table 3, for transitions between the initial and final JM states, with zero splitting in case of pairs containing a j = 0 state molecule (2. and 3.column in Table 3), and with the combined local splitting energies otherwise (4.column in Table 3). An averaged frequency of each pair transition band can be finally calculated giving an effective shift which is shown in the 5. column of Table 4. Gaussian profiles used for the contributions of the quite many J'M'← JM transitions are certainly a rough assumption, but considerable computational efforts are needed to properly combine the local rigid-lattice splitting with the intial and/or final $H_2$ pair - exciton interaction integrated over the lattice. The emission rates $A_{if}$ calculated by using Eqs. 26 and 27 are printed in the 6. column of Table 4. The calculated emission profile is finally expressed in Jansky units ($10^{-30}$ watt $cm^{-2}$ $Hz^{-1}$) for the comparison with the measurement and multiplied with an appropriate scaling factor fitted to the observed band intensity as shown in Figure 2. The resulting observed flux intensity in Watt/$cm^2$ units is shown in the 7.column of Table 4.

The fitted zero-phonon bands are used to determine pair column densities of the source. The SWS aperture has been 14×20 $arcsec^2 \equiv 6.5812 \cdot 10^{-9}$sr. Assuming a source distance of 440 parsec ($1.3574 \cdot 10^{19}$m), it spans an area of $\approx 1.2 \cdot 10^{30}$ $m^2$. The flux density corrected for the aperture and the emission rate $A_{if}[sec^{-1}]$ determine the (averaged) column density of the observed pair transition to be $N = 4\pi\lambda$ Flux/(hc$A_{if}$) [$cm^{-2}$]. Estimates are shown in the 8.column of Table 4. Filling factors of the sources are unknown.

This is in my opinion the presently possible and successful handling of the seven pure parahydrogen pair transition bands contributing to the four features. In contrast to this result, the transition frequencies of three bands of mixed ortho-para pairs cannot be shown in agreement with measured single transition frequencies, and their profiles are unknown,

Table 3: Lower and upper bounds of the local splitting of initial and/or final M states into JM states as calculated from Eqs. 7 and 9 (in wavenumbers), and maximum combined energy differences of initial and final JM states in transitions.

| transitions | initial (Eq.8) | final (Eq.9) | combined |
|---|---|---|---|
| (3, 2) → (1, 0) | -1.9 to +2.5 | | |
| (6, 0) → (4, 2) | | -1.0 to +0.4 | |
| (4, 2) → (2, 0) | -3.4 to +4.9 | -1.7 to +1.2 | -4.6 to +6.6 |
| (6, 2) → (4, 2) | -2.2 to +2.6 | -6.4 to +3.6 | -5.9 to +9.0 |
| (8, 0) → (6, 2) | | -0.1 to +0.1 | |
| (5, 2) → (3, 0) | -2.2 to +2.5 | | |
| (3, 4) → (1, 2) | -0.3 to +0.2 | -2.0 to +2.8 | -2.3 to +3.2 |
| (6, 2) → (4, 0) | -2.3 to +2.6 | | |
| (4, 4) → (2, 2) | -2.0 to +3.0 | -1.2 to +2.5 | -4.0 to +2.3 |
| (10,0) → (8, 2) | | -0.1 to +0. | |

Table 4: Calculated and fitted parameters of the zero-phonon bands (ordered in frequency)

| | band in v = 0 | [$cm^{-1}$] | width [$cm^{-1}$] | shift [$cm^{-1}$] | $A_{if}$ [$sec^{-1}$] | flux [$Wcm^{-2}$] | N [$cm^{-2}$] |
|---|---|---|---|---|---|---|---|
| I | S(1)+S(0) | 941.47 exp | | ≈ -54.6 | 4.62e-6 | 3.69e-18 | 8.63e+16 |
| | S(4)–S(0) | 887.84 exp. | 20.0 | -0.06 | 2.47e-6 | 2.59e-18 | 1.14e+17 |
| II | S(2)+S(0) | 1167.1 exp. | 40.0 | -1.05 | 3.94e-5 | 9.25e-18 | 1.94e+16 |
| | S(4) | 1243.44 exp. | 40.0 | +1.31 | 7.92e-6 | 5.98e-18 | 5.84e+16 |
| | S(6)–S(0) | 1278.18 exp. | 20.0 | +0.08 | 7.36e-6 | 5.08e-18 | 5.19e+16 |
| III | S(3)+S(0) | 1389.14 exp | 32.0 | ≈ -73.8 | 1.30e-5 | 1.26e-17 | 7.06e+16 |
| | S(1)+S(2) | 1396.9 exp | 32.0 | ≈ -46.8 | 2.13e-5 | 5.73e-18 | 1.91e+16 |
| | S(4)+S(0) | 1599.04 exp. | 20.0 | -0.01 | 4.29e-5 | 4.26e-18 | 5.97e+15 |
| IV | S(8)-S(0) | 1612.5 | 20.0 | | 1.45e-5 | 4.22e-18 | 1.74e+16 |
| | S(2)+S(2) | 1623.00 exp. | 40.0 | -0.09 | 5.02e-5 | 4.67e-18 | 5.51e+15 |

certainly not Gaussian. As a matter of fact, the unknown initial excess binding energies of the three mixed ortho-pare pair transition bands can only be estimated by fitting band positions to the measured features. The fits of the bands are now briefly discussed in detail.

The lowest possible transition frequency of the double de-excitation series belongs to the 0-0 S(0) + 0-0 S(0) band ($\Delta\nu \approx 12$ B). It is omitted. Fig.1 does not show any weak band of 40 - 45 $cm^{-1}$ width at about 710 $cm^{-1}$. I explained in section 2 that the parahydrogen ground-state pairs occur only with positive parity because of the required symmetrization of the parahydrogen wave functions, i.e., emission from the initial pair of two j = 2 state molecules with $l = 0$, meaning positive parity, is forbidden. It helps higher rotational-vibrational states of $H_2$ in the solid to relax in double rotational transitions by means of S(0) excitons. (In contrast to this, S(0) + S(0) absorption is allowed because the angular momentum j defined by $|j_1 - j_2| \leq j \leq j_1 + j_2$ allows non-zero wave functions with combinations of odd js and (odd) $l = 3$).

The next step of double rotational de-excitations, S(1) + S(0), marked no. I in Table 2, is a mixed ortho-para pair transition with an estimated downward band shift of ≈ -55.$cm^{-1}$, the excess binding energy produced by the ortho-$H_2$ j = 3 state in local distortion, interacting with the delocalized j = 2 state molecule in the parahydrogen lattice. Figure 2 shows two bands fitted to the measured feature at roughly the same energy, with unknown real portions of flux contributed from the two transitions. As we will see later on, I may argue in favor of the S(4) - S(0) band being the better candidate for a treatment with Gaussian contributions at the experimental transition frequency of the pair. At most a very small extra frequency shift for the pure parahydrogen band is realistic. The remaining intensity is left to the S(0) + S(1) band and a plausible rest is left to the phonon wings, especially on the blue side.

Feature II can be explained most probably with only one double de-excitation band of the de-excitation series, the S(2) + S(0) band, with an averaged transition frequency of 1166.05 $cm^{-1}$ (≈ 20 B) which comes close to the sum of the experimental transition frequencies of the pair. The initial and final j = 2 states of the transition produce about twice the effective width of ≈ 20 $cm^{-1}$. It is worth noting that both the initial and the final pair state contribute to the local rigid-lattice splitting: the final ($j_1$', $j_2$') = (0,2) pair state as shown in detail in section 3, Eqs.10ff, but with $l = 3$, and the initial state with both terms of the symmetrized angular part of the wave function (Eq.3 in section 2). The combined local rigid-lattice splitting gives more than 11 $cm^{-1}$. The position of the band fits properly to the measured feature which may be understood as a not too bad application of the Gaussian profiles and of a negligible shift of the initial ($j_1$, $j_2$) = (4,2) pair state which could be a result of the spin-lattice coupling of the j = 4 state.

The pure ortho-$H_2$ 0-0 S(1) + 0-0 S(1) pair transition belongs to the general series at about the same frequency, but it does not contribute to the observed spectrum which confirms the assumption of a small ortho-para ratio and small abundances of rotationally excited ortho-$H_2$ pairs. It could emit with a different band width compared to the other bands and with lower intensity because of missing excitons.

The background intensity between feature II and the lowest frequency band of feature III needs an extra band fit. There is no double rotational transition available at this position and, as far as I know, there is no peak showing up at any other source in the frequency range between features II and III. A single S(4) transition with a delocalized j = 2 companion is in the right frequency position and contributes with the estimated band width of the j = 2 state extended by a combined local splitting of 14.9 $cm^{-1}$. More single transitions in the crystal will be discussed in the next section.

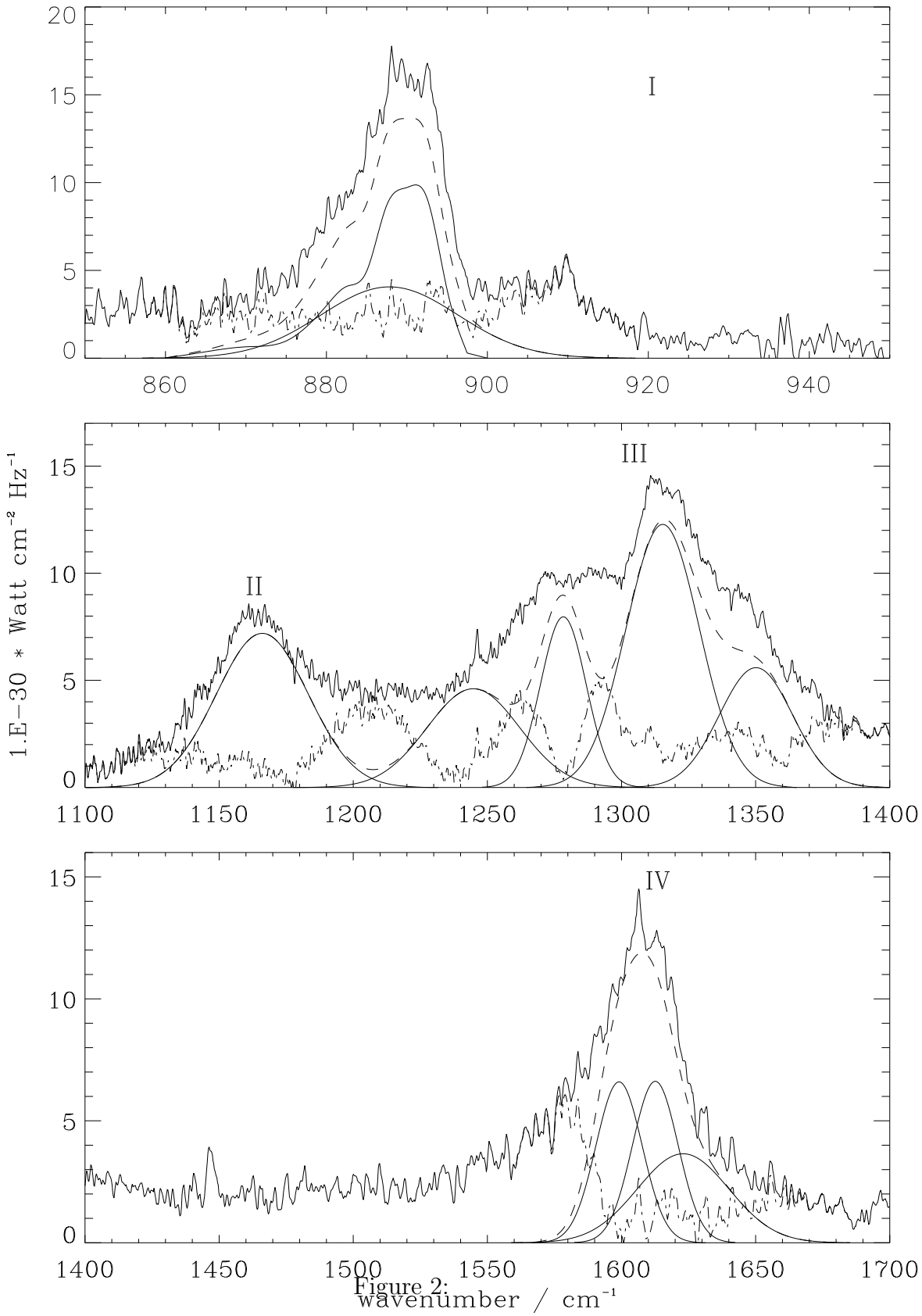


Figure 2:

The first band in feature III, again a de-excitation plus excitation band, seems to be slightly uncertain with regard to total width and frequency position. There is too much unexplained flux left on the red side. A solution to this problem could be found in a correction of the band position of about 3 to 4 $cm^{-1}$ resulting from the self-energy of the j = 8 state molecule.

Feature III is dominated by the two mixed ortho-para double rotational pair transitions S(3) + S(0) and S(1) + S(2). The former shows a relatively small initial EQQ splitting, but the stronger excess binding energy shift because of the delocalized initial j = 2 state. Both combine initial and final local rigid-lattice splitting with the delocalized j = 2 splitting. As we can see in Fig.2, the shift of the latter could be uncertain by as much as roughly $\pm$ 10 $cm^{-1}$. Both bands are fitted with 32 $cm^{-1}$ widths and invalid Gaussian profiles. The Gaussian profiles have been used simply because nothing is known about the real profiles and how the intensities of the two bands are assessed in reality. Only the emission rates are valid data comparable in quality to the emission rates of the pure parahydrogen bands.

The three bands of feature IV are again pure parahydrogen double rotational transitions, two pertaining to the general series with a frequency of about 28 B. The pure ortho-$H_2$ pair transition S(1) + S(3) belongs to the same frequency range, but it is also neglected in the analysis of the spectrum, for the same reasons as mentioned above in the discussion of feature II. A slightly better fit of this feature could be done, if the S(4) + S(0) band position could be shifted to the red side, maybe by 3 to 4 $cm^{-1}$, again as a result of an effective self-energy of the initial j = 6 state. The splitting of the final pair state of the S(2) + S(2) band gives the same results as for the double rotational absorption from ground-state pairs. A complete fit of feature IV should also contain a small contribution of a single S(6) transition, again with a delocalized j = 2 companion.

# 6. Summary and Discussions

Zero-phonon bands of solid hydrogen have been calculated in the wavelength range between 6 and 12 $\mu$m by applying Van Kranendonk's approximate method of $H_2$ pairs in a rigid lattice. The obtained results have been fitted to the features of the ISO-SWS spectrum observed at the NGC7023 nebula, a well-known PDR.

The pair approximation is based on the fact that interactions in the lattice are appropriately described by the sum over pair interactions between the lattice molecules. This assumption is valid also for the dipole moment function mainly determined by the sum over all quadrupole induced dipoles.

Cancellation effects valid in the hcp crystal reduce the interaction potential of $H_2$ pairs to the essential electric quadrupole-quadrupole (EQQ) interaction term $V_{224}$, minor important terms are neglected, and the same crystal symmetry effects reduce the pair dipole moment function to the essential quadrupole induction term $D_{2233}$ in the spherical expansion. The EQQ interaction causes level splitting of the total angular momentum J states of two rotating molecules at nn distance which has been calculated and applied in calculations of the $|JM>$ dipole transitions.

Basic symmetry properties are required for the zero-order pair wave functions because the $H_2$ molecules are Bose particles, i.e., pair wave functions of pure parahydrogen must be symmetric, and the interaction potential between identical (indistinguishable) para-$H_2$ molecules obtained for the symmetrized pair wave functions is generally symmetric in

both directions. This symmetry does not apply to mixed ortho-para $H_2$ pairs because ortho-$H_2$ and para-$H_2$ molecules are distinguishable, i.e., their pair wave function is not symmetrized, resulting in radially directed forces between the single ortho-$H_2$ molecule in the middle and the twelve nn molecules around, the general reason of excess binding energies of the rotationally excited single ortho-$H_2$ molecules in the parahydrogen crystal.

The forbidden S(0) + S(0) emission in the pair approximation applied to the solid is also a property determined by basic symmetry requirements of parahydrogen pairs in the solid, whereas it is an allowed (and observed) transition in absorption because of the existing final j = 1 and 3, $l = 3$ pair states. The zero orbital angular momentum of the initial state is assumed as a plausible solid-state property of hydrogen, and the odd ($l = 3$) orbital angular momentum of the final state is a consequence of the zero-phonon pair approximation and is required by the leading dipole moment term $D_{2233}$. I may note that a significant emission band observed at about 710 wavenumbers would be proof against the applied pair approximation of the zero-phonon bands, at least against the assumed $l = 0 \rightarrow 3$ transition of the orbital angular momentum, It would probably mean a contribution from a different source. The other way round, the missing emission band at the S(0) + S(0) transition frequency is a gratifying little detail contributing to the evidence of solid hydrogen emission.

The widths and the intensity of the dipole pair transition bands used in the analysis of the observed spectrum are mainly determined by delocalized j = 2 state molecules participating in the pair states. I have briefly indicated in section 3 that the wave function of the delocalized j = 2 state fulfills the requirement of the Bloch theorem, but I did not proceed with calculations to evaluate the energy spread of it. Instead, I accepted the estimated value obtained by Van Kranendink [2] to be applied in the fits of the observed spectrum, meaning a width of the rotational pair transition bands of $\approx 20$ cm$^{-1}$ for each j = 2 state contained in the pairs initially and/or finally. As to the generally found constant widths of the features observed at practically all sources, the proper widths of the pair transition bands used to explain the features contribute particular details to the spectroscopic evidence.

The crucial role of the delocalized j = 2 state in the fit of the prominent features between 6 and 12 $\mu$m is intensified by the second important value accepted from Van Kranendonk's calculations, the lattice sum over the squared matrix elements of the rotational pair transitions. It works as an enhancement factor of the emission rates for each j = 2 state starting or ending in the rotational pair transitions. Hence only rotational pair transition bands with participating j = 2 states have been used to fit all observed prominent features, and vice versa, all rotational pair transition bands with participating j = 2 states have been used which fall into the frequency range of the prominent features.

Spin-lattice coupling has been assumed to be fast when the orbiting energy of $l = 3$ of the final pair state (14.27 cm$^{-1}$ at nn distance) has to be immediately transferred into phonon intensity. In contrast to this minor energy offer to the lattice, it is assumed (also by Van Kranendonk [2], sec.6), that the migration of the rotationally excited ortho-$H_2$ impurities is slow, too slow to cause a significant energy shift in absorption, as experiments show (see the S(0) + S(1) absorption band in Fig.4 in Balasubramanian et al. [20]), but in view of the small emission rates fast enough to be already finished before emission. As a result we find significant deviations of the mixed-pair transition frequencies in emission compared to absorption. Small shifts of the order of a few wavenumbers caused by self-energies of the higher rotationally excited para-$H_2$ molecules seem to appear in the fit of the bands, but they have been neglected in the plots shown in Fig.2.

I may summarize the results of this paper as follows. It has been found that the

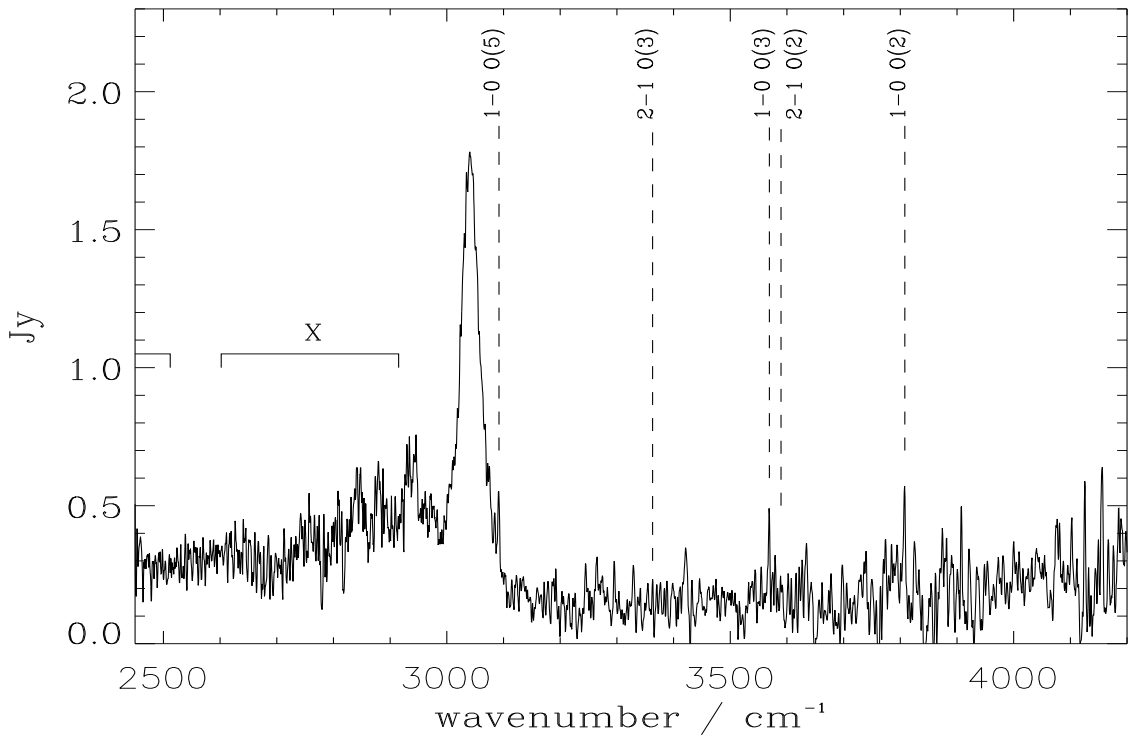


Figure 3:

frequency positions and the widths of six pure parahydrogen pair transition bands used to explain the observed features fit with sufficient accuracy in favor of spectroscopic evidence of solid hydrogen radiation. In contrast to this, the correct frequency positions of the also contributing three mixed ortho-para pair transition bands are unknown. They need further computational efforts to determine the quantitative local distortions around single ortho-$H_2$ impurities and the excess binding energies of the initial pair states. Again the EQQ interaction and the delocalized j = 2 states will play the dominant role in these attempts. The success found for the pure parahydrogen bands promises success also for the remaining mixed ortho-para $H_2$ bands.

The significant zero-phonon bands are all explained by double rotational pair transitions, either twofold de-excitations or single de-excitations combined with single excitations. But the 3-j Wigner symbols in Eq.22 allow also single rotational transitions in pairs with a rotating companion at nn distance. Two bands of this type have been mentioned in the fit of the prominent features. One could speculate eventually also on a single S(2) transition with a j = 1 companion slightly below 800 wavenumbers: assumed an excess binding energy of $\approx 20$ cm$^{-1}$ for the j = 1 state (with local distortions enhanced by the j = 4 state), the pair transition energy comes close to the feature at $\approx 790$ wavenumbers observed in the ISO-SWS mission. Even a single S(0) transition is possible with any rotating companion. Plausible emission bands like these are waiting for experimental verification.

Continuation of the general series of double rotational transitions to higher frequencies is of interest. As to my knowledge, the following feature V in the series does not show

prominent peaking bands of $\approx$ 20 cm$^{-1}$ width, but a general background of radiation at frequencies above the 1600 wavenumbers of feature IV. This is plausible because the frequency gap between the mixed ortho-para bands as well as the portion of the phonon branches increases. There is a general tendency above feature IV of inceasing frequency gaps between the leading zero-phonon bands of the higher j transitions. This can be shown for the pure parahydrogen pair transitions of feature VI. The frequency positions of zero-phonon bands of feature VI are known, i.e., a few wavenumbers smaller than 1913 cm$^{-1}$ for the S(10) – S(0) band, close to 1989 cm$^{-1}$ for the S(0) + S(6) band and close to 2055 cm$^{-1}$ for the S(2) + S(4) band. Unfortunatly, the available ISO-SWS spectrum of the NGC7023 nebula is too noisy between 1800 and 2500 cm$^{-1}$ and cannot be used for a fit. For a serious attempt of fitting feature VI one would need a qualified spectrum observed at a different source. The amplitudes of the three bands of feature VI should be less prominent because of decreasing column density of the de-excitation plus excitation band S(10) – S(0), possible increasing portions of phonon branches and because the rotational states j = 6 and 8 contribute also to the emission features I, III and IV with high column densities. The weakly exposed bands with their phonon branches make Doppler profiles as used in this paper really inappropriate for a fit procedure.

Transitions from rotational states higher than j = 13 are hardly contributing significantly to observable solid hydrogen radiation because the general series ends with features X and XI containing j = 12 and 13 as the highest initial rotational states, and the two last features are obviously mixed up below 3000 cm$^{-1}$ (Fig.3).

Another type of double rotational transitions starts up above 3000 cm$^{-1}$: the O + S series. In front of those we have a special type of feature at 3040 cm$^{-1}$ and below this frequency. It should be O de-excitations plus S(0) excitation, i.e., the lowest rotational state in $v \neq 0$ is reached in the relaxation process, and the rotational excitation of a ground-state molecule at nn distance is needed for a double rotational transition. The widths and shifts of these bands are unknown. More work is needed on this subject. One can also speculate on possible effects of a combined roton-vibron exciton, the 1-0 S(0) exciton in parahydrogen solids, but this is above the frequency range of the ISO mission.

Finally I wish to express my hope that more experimental work on solid hydrogen will be initiated with the results shown in this paper. I have been told that the technology needed for emission measurements is available. And in return, attempts of improved theoretical work will certainly be initiated, when frequency resolved laboratory measurements of the emission bands of interest become available.

## Acknowledgment

I am grateful to H. Feuchtgruber from the MPE who proposed the ISO-SWS spectrum of the NGC7023 nebula to be analysed and helped me to the measured spectra used in the paper.

## References

[1] F. Boulanger, P. Boissel, D. Cesarsky, C. Ryter, A&A 339 (1998) 194, and additional papers cited therein.
[2] J. Van Kranendonk, Solid Hydrogen, Plenum Press, N.Y., 1983
[3] H.P. Gush, W.F.J. Hare, E.J. Allin, H.L. Welsh, Phys.Rev. 106 (1957) 1101

[4] H.P. Gush, W.F.J. Hare, E.J. Allin, H.L. Welsh, Can.J.Phys. 38 (1960) 176
[5] E.J. Allin, H.P. Gush, W.F.J. Hare, H.L. Welsh, Nuovo Cimento Suppl. 9 (1958) 77
[6] Z.J. Kiss, PH.D. thesis, University of Toronto, Toronto, Ontario, 1959
[7] J. Van Kranendonk, Physica 25 (1959) 1080
[8] J. Van Kranendonk, Can.J.Phys. 38 (1960) 240
[9] J.D. Poll, J. Van Kranendonk, Can.J.Phys. 40 (1962) 163
[10] J. Van Kranendonk, G. Karl, Rev.Mod.Phys. 40 (1968) 531
[11] A.P. Mishra, T.K. Balasubramanian, R.H. Tipping, Q. Ma, J.Mol.Structure 695 (2004) 103
[12] J. Schaefer, W.E. Köhler, Z.Phys.D - Atoms, Molecules and Clusters 13 (1989) 217
[13] A.R. Edmonds, *Drehimpulse in der Quantenmechanik*, Hochschultaschenbücher-Verlag, 1964
[14] S. Flügge, Handbuch vol. XLII, p. 544
[15] M. Mengel, B.P. Winnewisser, M. Winnewisser, J.Mol.Spectr. 188 (1998) 221
[16] J. Van Kranendonk, V.F. Sears, Can.J.Phys. 44 (1966) 313
[17] S. Luryi, J. Van Kranendonk, Can.J.Phys. 57 (1979) 933
[18] K. Takayanagi, Adv.At.Mol.Phys. 1 (1965) 149
[19] J.L. Hunt, J.D. Poll, L. Wolniewicz, Can.J.Phys. 62 (1984) 1719
[20] T.K. Balasubramanian, C.-H. Lien, J.R. Gaines, K. Narahari, E.K. Damon, J.Mol.Spectr. 92 (1982) 77
[21] J.C. Raich, L.B. Kanney, J.Low Temp.Phys. 28 (1977) 95
[22] R.H. Tipping, J.D. Poll, Molecular Spectr.: Modern Research, vol.III, (1985) 421
[23] B.R.A. Nijboer, F.W. De Wette, Physica XXIII, (1957) 309
[24] E.U. Condon, G.H. Shortley, The Theory of Atomic Spectra, Cambridge University Press 1967
[25] T.K. Balasubramanian, C.-H. Lien, K. Narahari Rao, J.R. Gaines, Phys.Rev.Lett. 47 (1981) 1277
[26] U. Bountempo, S. Cunsolo, P. Dore, L. Nencini, Can.J.Phys. 60 (1982) 1422
[27] M. Okomura, Man-Chor Chan, T. Oka, Phys.Rev.Lett. 62 (1989) 32
[28] R.A. Steinhoff, B.P. Winnewisser, M. Winnewisser, Phys.Rev.Lett. 73 (1994) 2833

**Figure Captions**

Figure 1: The ISO-SWS spectrum of the NGC7023 nebula has been observed with an aperture of 14×20 arcsec$^2$ ($6.5812 \cdot 10^{-9}$ steradian) at Galactic l = $104.061617^o$, b = $14.1927^o$. Gas phase emission lines are marked with vertical dashed lines and identified in the upper row above the spectrum. The features above 800 cm$^{-1}$, marked I – IV, are explained and identified as rotational transition bands of hydrogen pairs emitted in solid hydrogen.

Figure 2: The prominent features of the ISO-SWS spectrum, observed in the NGC7023 nebula, are fitted by means of zero-phonon bands emitted in solid hydrogen, at experimentally determined frequency positions only in the case of pure parahydrogen pairs, at estimated positions otherwise, with band widths mainly determined by the estimated effect of delocalized j = 2 states and added local splittings of the initial and final $|JM>$ pair states, and with calculated emission rates enhanced by the estimated lattice sum over delocalized j = 2 states. The measured spectrum and the fitted bands are plotted with solid lines, combined intensities of the bands are shown with dashed lines, and the rest radiation intensity is plotted with the dotted-dashed curve; it is assumed to be mainly from phonon radiation. Quantitative details of the bands are shown in Table 4 and discussed in the text.

Figure 3: The ISO-SWS spectrum of the NGC7023 nebula observed with 14×20 arcsec$^2$ aperture showing the low-density gas phase vibrational-rotational lines of $H_2$ (labeled above the spectrum) emitted in the PDR, the upper end of the solid-state double-rotational band series at about 3000 cm$^{-1}$, the peak at 3040 cm$^{-1}$ explained by means of de-excitation plus excitation bands, and part of the solid-state S + O transitions starting above this peak. The estimated spread of the bands contributing to series number X is included.